remote sensing

MDPI

Article

The Relative Contributions of Climate and Grazing on the Dynamics of Grassland NPP and PUE on the Qinghai-Tibet Plateau

Huilin Yu, Qiannan Ding, Baoping Meng, Yanyan Lv, Chang Liu, Xinyu Zhang, Yi Sun, Meng Li * and Shuhua Yi

School of Geographic Sciences, Nantong University, Nantong 226007, China; 2017320004@stmail.ntu.edu.cn (H.Y.); 1822011046@stmail.ntu.edu.cn (Q.D.); mengbp09@lzu.edu.cn (B.M.); lvyy18@ntu.edu.cn (Y.L.); 1921110165@stmail.ntu.edu.cn (C.L.); 1822011018@stmail.ntu.edu.cn (X.Z.); sunyi@ntu.edu.cn (Y.S.); yis@ntu.edu.cn (S.Y.)

* Correspondence: limeng@ntu.edu.cn

Abstract: Net primary productivity (NPP) and precipitation-use efficiency (PUE) are crucial indicators in understanding the responses of vegetation to global change. However, the relative contributions of climate change and human interference to the dynamics of NPP and PUE remain unclear. During the past few decades, the impacts of climate change and human activities on alpine grasslands on the Qinghai-Tibet Plateau (QTP) have been intensifying. The aims of the study were to investigate the spatiotemporal patterns of grassland NPP and PUE on the QTP during 2000–2017 and quantify how much of the variance in NPP and PUE can be attributed to the climatic factors (precipitation and temperature) and grazing intensity. The results showed that: (1) grassland NPP significantly increased with a rate of 0.6 g C m^{-2} $year^{-1}$ over the past 18 years, mainly induced by the increased temperature and the enhanced precipitation. The temperature was the dominant factor for NPP interannual variation in mid-eastern QTP, and precipitation restrained vegetation growth most in the southwest and northeast. (2) The PUE was higher on the eastern and western parts of the plateau, but lower at the center. Regarding grassland types, the PUE of alpine steppe (0.19 g C m^{-2} mm^{-1}) was significantly lower than those of alpine meadow (0.31 g C m^{-2} mm^{-1}) and desert steppe (0.32 g C m^{-2} mm^{-1}). (3) Precipitation was significantly and negatively correlated with PUE and contributed the most to the temporal variation of grassland PUE on the QTP (52.7%). (4) Furthermore, we found that the grazing activities had the lowest contributions to both NPP and PUE interannual variation, compared to temperature and precipitation. Thus, it is suggested that climate variability rather than grazing activities dominated vegetation changes on the QTP.

Keywords: alpine grassland; carbon and water cycles; climate change; human activities; Tibetan Plateau

Citation: Yu, H.; Ding, Q.; Meng, B.; Lv, Y.; Liu, C.; Zhang, X.; Sun, Y.; Li, M.; Yi, S. The Relative Contributions of Climate and Grazing on the Dynamics of Grassland NPP and PUE on the Qinghai-Tibet Plateau. *Remote Sens.* **2021**, *13*, 3424. https://doi.org/10.3390/rs13173424

Academic Editors: Adrian Ursu and Cristian Constantin Stoleriu

Received: 5 August 2021
Accepted: 26 August 2021
Published: 28 August 2021

1. Introduction

Due to climate change and human activities, terrestrial ecosystems have undergone unprecedented changes, including the changes of carbon sources and sinks [1], land cover and land use [2–4], and loss of biodiversity [5]. The human–climate–vegetation interaction has become one of the major environmental paradigms [6,7]. Particularly in arid and semi-arid regions, anthropogenic activities and climate change can easily cause ecosystem degradation [8]. The grassland ecosystem is one of the most widely distributed vegetation types, accounting for about one-fifth of the world's surface area [9]. It plays a vital role in maintaining biogeochemical cycles, protecting biodiversity, and supporting animal husbandry and food production [10]. Due to global warming and overgrazing, nearly 50% of global grasslands have degraded [11]. Grassland degradation is threatening many habitats and even affecting ecological security. Although the dynamics of grasslands have been explored by intensive studies, the studies on relative contributions of climatic and anthropogenic drivers in influencing grassland variations are limited.

Net primary productivity (NPP) represents the amount of carbon fixed by plants in-a certain period of time and characterizes the energy production and conversion status [12,13]. Precipitation-use efficiency (PUE) is the ratio of NPP to precipitation, and reflects the relationship between energy production and water consumption [14]. NPP and PUE are essential indicators for the relationship between terrestrial water and carbon cycles [15]. NPP is positively correlated with precipitation in almost all terrestrial ecosystems [16], particularly in grassland ecosystems [17]. Accelerated warming can also promote NPP by prolonging the growing season [18,19]. PUE is generally considered to decrease with spatial precipitation [15]. It has also been suggested that PUE decreases from arid biomes to humid biomes, changing with the level of precipitation [20]. Meanwhile, human activities can profoundly affect vegetation changes and even cause detrimental or catastrophic damage to plant growth [21]. For example, overgrazing could lead to decreased vegetation productivity and trigger severe grassland degradation [22,23]. Therefore, understanding how NPP and PUE respond to climate and grazing is essential for mitigating environmental damages.

The Qinghai-Tibet Plateau (QTP) is the highest Plateau in the world, with an average elevation of higher than 4000 m. Alpine grasslands cover most areas of the QTP and feature fragile environmental conditions [24,25]. The air temperature has increased about twice as fast as the global average during the past three decades [26], and the livestock number almost tripled in the 1990s from the 1950s [27]. The dramatic climate change and intensive grazing activities have caused half of the grasslands to degrade [28]. Recently, studies on how climate change and human activities influence the changes in NPP or PUE on the Tibetan Plateau are emerging. For example, Chen et al. [29] found that human activities dominated the NPP variations after 2001, and Lehnert et al. [30] suggested that climate variability was the primary driver for NPP changes. In terms of PUE, Yang et al. [31] stated that spatial PUE in Tibetan grasslands exhibited a unimodal pattern across broad precipitation gradients. However, Zhao et al. [32] argued that the spatial PUE had a U-shaped relationship with precipitation. These differences may be caused by the different climate gradients and human activity intensity levels [32]. Therefore, it is important to identify the spatiotemporal changes of NPP and PUE across the QTP and quantify the relative contributions of the climate factors and human activities to their dynamics.

The study aimed to answer: (1) How did grassland NPP and PUE vary from 2000 to 2017? (2) How much can the variances in NPP and PUE be attributed to the corresponding climatic factors and grazing intensity, respectively? To answer these questions, firstly, we simulated grassland NPP and PUE across the QTP from 2000 to 2017 and explored the changes in climatic factors (precipitation and temperature) and in grazing intensity over time. Secondly, we investigated the relationships of NPP and PUE with temperature, precipitation, and grazing intensity. Finally, we quantified the relative importance of climate and grazing to influencing interannual NPP and PUE variations.

2. Materials and Methods

2.1. Study Area

The QTP is located in southwestern China and accounts for more than 26.8% of the total land area of China (Figure 1a). Known as the "roof of the world" and the "Asian water tower", this plateau is a crucial security barrier for China and even Asia [33]. The QTP lies in the alpine zone and has a mean annual temperature below 0 °C. The distribution of precipitation is uneven. The mean annual precipitation is greater than 1000 mm in the southeastern plateau and less than 100 mm in the northwestern part [34]. These unique climatic conditions have developed various alpine ecosystems on the QTP. The grasslands are mainly composed of humid alpine meadow, semi-arid alpine steppe, and arid desert steppe (Figure 1b). The grassland areas on the QTP cover 1.3×10^8 hectares, accounting for about 32.5% of the grassland area in China [35]. Herders have existed on rgw QTP for tens of thousands of years, and livestock husbandry is their primary source of income [26].

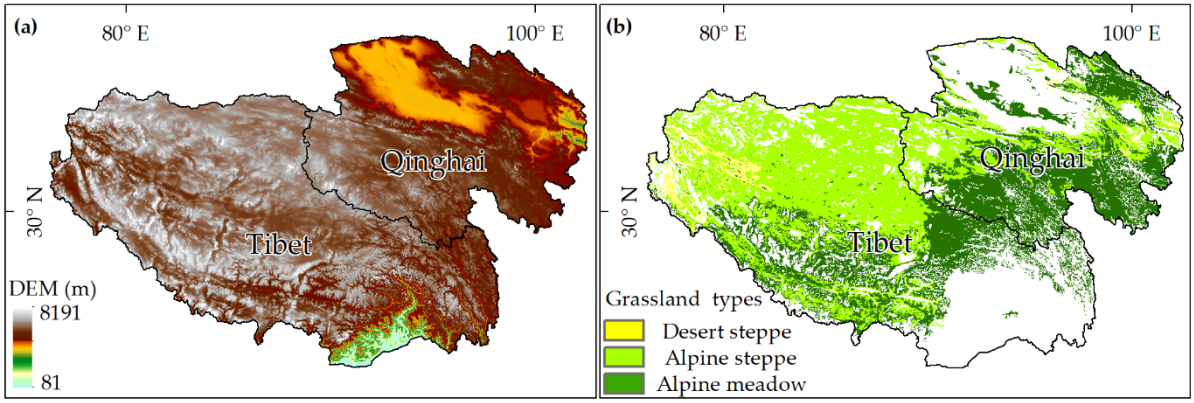

Figure 1. (**a**) The altitude of the study region and (**b**) the spatial pattern of the grassland types. DEM indicates digital elevation model.

2.2. Data Collection and Process Method

The monthly MOD13A3C6 normalized difference vegetation index (NDVI) data were obtained from the NASA LP DAAC (Land Processes Distributed Active Archive Center) website (https://lpdaac.usgs.gov/get_data/data_pool, accessed on 1 May 2020). This dataset were calculated by the maximum value composite method at a 1000 m resolution and calibrated for geometrical, atmospheric, and radiation influences. The MODIS Reprojection Tool (MRT) was used to define geographical coordinates as WGS1984 and the projection coordinate as Albers conical equal area projection [36]. The NDVI data were handled with the TIMESAT software further to eliminate the effects of clouds and atmospheric contamination. This is a software package for processing and assessing the time-series data of vegetation dynamics, and curve fits and runs phenological/seasonality metrics [37,38]. Based on an asymmetric Gaussian function-fitting, we adopted the Savitzky–Golay (SG) smoothing model to eliminate the influence of random noise, using data filtering and reconstruction [39].

The meteorological data, including daily temperature, precipitation, and sunshine duration, were downloaded from the National Meteorological Information Center of China Meteorological Administration (http://geodata.cn, accessed on 1 May 2020). The radiation was calculated based on geographical position and sunshine duration [40]. Firstly, the daily climatic data were integrated into monthly data. Then, ANUSPLIN4.3 was used to interpolate monthly precipitation, temperature, and radiation into the raster with a spatial resolution of 1000 m [41].

Socio-economic data with livestock numbers from 2000 to 2017 were obtained from statistical yearbooks for the Tibet Autonomous Region and Qinghai province. We collected livestock inventory and the number of livestock slaughtered for each county on the QTP. Different types of livestock animals were converted to standard sheep units (SHU) based on a method in which one sheep or one goat is equal to one SHU, and one large livestock animal (yak, donkey, and horse) is equal to four SHUs [42]. Grassland distribution was determined by the China Vegetation Atlas with a scale of 1:1,000,000, which was derived from the Resource and Environment Data Cloud Platform (http://www.resdc.cn/data.aspx?DATAID=122, accessed on 1 May 2020).

2.3. NPP Simulation and Validation

Along with the development of remote sensing techniques and geographic information systems, some models based on light use efficiency (LUE) and remote sensing data were well developed to study NPP and estimate carbon dynamics at global or regional scales. Monteith et al. [43] and Potter et al. [44] found that vegetation productivity is correlated with the amount of photosynthetically active radiation absorbed or intercepted by green foliage and then built CASA (Carnegie–Ames–Stanford approach) model. The CASA runs on a monthly time interval to model the seasonal carbon cycle. In recent decades, this

model has been modified by many researchers [45–47]. In CASA, NPP on grid cell x in month t is determined by absorbed photosynthetically active radiation (APAR) and the actual LUE (ε). The formulas are as follows:

$$NPP(x, t) = APAR(x, t) \times \varepsilon(x, t) \quad (1)$$

$$APAR(x, t) = SOL(x, t) \times FPAR(x, t) \times 0.5 \quad (2)$$

where x is spatial location; t is time; SOL is total solar radiation MJ/m^2 at grid cell x in month t; 0.5 represents the ratio between photosynthetically active solar radiation and total solar radiation. FPAR is the fraction of photosynthetically active radiation absorbed by vegetation, which can be quantified by NDVI and vegetable types.

The light energy conversion (ε) is influenced by water and temperature. The calculation formula is:

$$\varepsilon(x, t) = T_{\varepsilon 1}(x, t) \times T_{\varepsilon 2}(x, t) \times W_{\varepsilon}(x, t) \times \varepsilon^* \quad (3)$$

$T_{\varepsilon 1}(x, t)$ and $T_{\varepsilon 2}(x, t)$ represent temperature stress. $T_{\varepsilon 1}(x, t)$ reflects the inherent biochemical limitations on photosynthesis in plants at very low and very high temperatures. $T_{\varepsilon 2}(x, t)$ represents the change of the light energy conversion rate when the temperature changes from the optimum temperature to a high or low temperature. $W_{\varepsilon}(x, t)$ represents the effect of available water conditions on the light energy conversion. $W_{\varepsilon}(x, t)$ gradually increases with the amount of water available in the environment [45,48]. ε^* indicates the maximum possible LUE under ideal conditions. At the global scale, the value of ε^* is 0.389 g C·MJ^{-1} [49]. However, ε^* showed significant differences among vegetation types [50]. For alpine grasslands on the QTP, ε^* can be fixed at 0.56 g C·MJ^{-1} according to the finding by Zhang et al. [51].

$$T_{\varepsilon 1}(x, t) = 0.8 + 0.02 \times T_{opt}(x, t) - 0.0005 \times T_{opt}(x, t) \quad (4)$$

$$T_{\varepsilon 2}(x, t) = 1.1814/\{1 + \exp[0.2 \times (T_{opt}(x, t) - 10 - T(x, t))]\}/\{1 + \exp[0.3 \times (-T_{opt}(x, t) - 10 + T(x, t))]\} \quad (5)$$

$$W_{\varepsilon}(x, t) = 0.5 + 0.5 \times EET(x, t)/PET(x, t) \quad (6)$$

where $T_{opt}(x, t)$ is the monthly average temperature when the NDVI reaches the highest value. If the temperature on grid cell x in month t is below −10 °C, $T_{\varepsilon 1}$ is equal to 0. PET refers to potential evapotranspiration (mm), and EET refers to estimated evapotranspiration (mm).

The performance of CASA model has been validated by observed NPP data in the previous study. We found that the simulated NPP matched well with the measurement [34,52].

2.4. PUE Calculation

PUE has been calculated in two common ways. First, according to PUE's definition, it was calculated directly by the ratio of NPP and precipitation [53]. Second, PUE was estimated based on the slope of the NPP–precipitation relationship [20]. We accepted the first method using the ratio of grassland NPP and corresponding precipitation (PPT) because this method has been widely used on the QTP [15,31]. The formula is as follows:

$$PUE = \frac{NPP}{PPT} \quad (7)$$

where PUE is precipitation use efficiency (g C m^{-2} mm^{-1}), NPP is net primary production (g C m^{-2}), and PPT is precipitation in one year (mm).

2.5. Grazing Intensity Calculation

Grazing intensity (GI) is usually calculated as the ratio of livestock number to natural grassland, and the formula is as follows:

$$GI = \frac{C_n + C_h}{A} \quad (8)$$

where C_n is the livestock inventory in a given year, and C_h is the number of livestock slaughtered in a given year. A represents the area of available natural grassland (ha) in each county.

2.6. Data Analysis

We took alpine grassland as the research object. Before further analysis, we eliminated the non-grassland pixels and null-value pixels due to unavailable livestock data in the center of QTP. These data are indicated by white color in the figures. We used the ordinary least squares (OLS) linear regression method to calculate the temporal trend in grassland NPP and PUE during 2000–2017 for each pixel. The spatial analysis was calculated by *raster package* (https://cran.r-project.org/web/packages/raster/index.html, accessed on 1 October 2020). The differences in NPP and PUE among different grassland types were analyzed by the analysis of variance (ANOVA) using *agricolae* package (https://cran.r-project.org/web/packages/agricolae/index.html, accessed on 1 October 2020). The Spearman correlation test was used to calculate the relationships of NPP and PUE with climate and grazing.

Recently, the correlation metrics [54], principal component analyses [27], and generalized linear model (GLM) [30] were used to discriminate the relative contributions of climate change and human activities to vegetation changes. Among them, the GLM is simple and widely recommended [30]. In this study, the relative contributions of grazing and climate change to the temporal dynamics of NPP and PUE in each pixel were decomposed from the GLM. In the GLM model, we selected NPP and PUE as response variablesl and mean annual temperature (MAT), mean annual precipitation (MAP), and grazing intensity (GI) as predictor variables. The percentage of NPP or PUE variance explained by each predictor variable in the GLM was interpreted as the contribution of each variable to NPP or PUE variation. All statistical analyses were performed in the environment R4.02 (https://www.r-project.org/) and mapped in ArcGIS 10.2 (ESRI, Inc. 380 New York Street Redlands, CA 92373 USA).

3. Results

3.1. Spatiotemporal Patterns of Climate Factors and Grazing Intensity

From 2000 to 2017, the MAT in the QTP increased significantly with a rate of 0.05 °C/year ($p < 0.01$) (Figure 2a), particularly in western Tibet and southwestern Qinghai Province (Figure 2b). The MAP also showed a slight but non-significant increasing trend at a rate of 1.8 mm/year ($p > 0.05$) (Figure 2c). However, the spatial pattern of MAP trend demonstrated heterogeneity across the plateau. MAP significantly increased in the northeast of the QTP, and non-significantly decreased in the south of the Plateau (Figure 2d). The mean GI of the QTP showed unimodal dynamics from 2000 to 2017. The highest GI was generated in 2007 (0.72 SSU/ha), and the lowest value occurred in 2016 (0.64 SHU/ha) (Figure 2e). Evident spatial variability of the GI trend was observed across the QTP. The GI decreased in the southwestern region but increased in the northeastern part (Figure 2f).

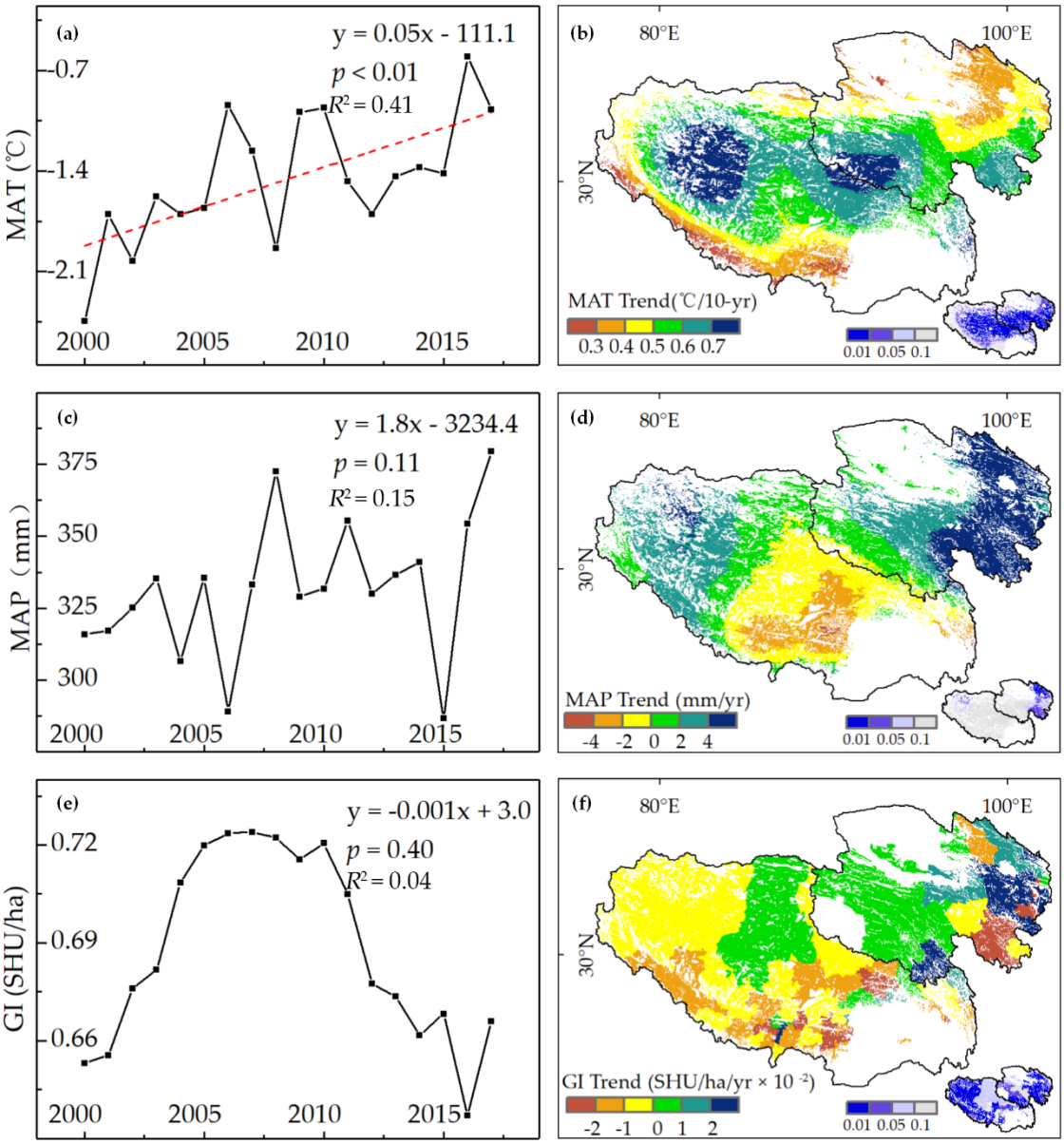

Figure 2. The spatiotemporal patterns of MAT (**a**,**b**), MAP (**c**,**d**), and GI (**e**,**f**) on the QTP from 2000 to 2017. MAT, MAP, and GI represent mean annual temperature, mean annual precipitation, and grazing intensity, respectively. Small maps at the bottom represent the ranges of significance levels.

3.2. Spatiotemporal Patterns of NPP

The overall mean annual grassland NPP during 2000–2017 on the QTP was 88.5 g C m^{-2}, and the highest and lowest NPP were found in 2010 (98.5 g C m^{-2}) and 2001 (80.7 g C m^{-2}), respectively. The spatial distribution of grassland NPP presented an increasing pattern from northwest to southeast of the QTP (Figure 3a). Alpine meadow on the southeastern plateau had the largest NPP (133.6 g C m^{-2}) due to the favorable hydrothermal conditions, followed by the alpine steppe (50.7 g C m^{-2}) and desert steppe (45.1 g C m^{-2}) (Table 1).

From 2000 to 2017, grassland NPP on the QTP increased significantly at a rate of 0.6 g C m^{-2} $year^{-1}$ (Figure 3a). Statistically, NPP significantly increased with 31.34% of grasslands, mainly in the north of the plateau. Grasslands with a significant decreasing trend in NPP only accounted for 0.68% of the total area. In different grassland types, 45.3% of desert steppe showed a significant increased trend in NPP, almost twice than that of alpine meadow and 1.5 times of alpine steppe (Table 1).

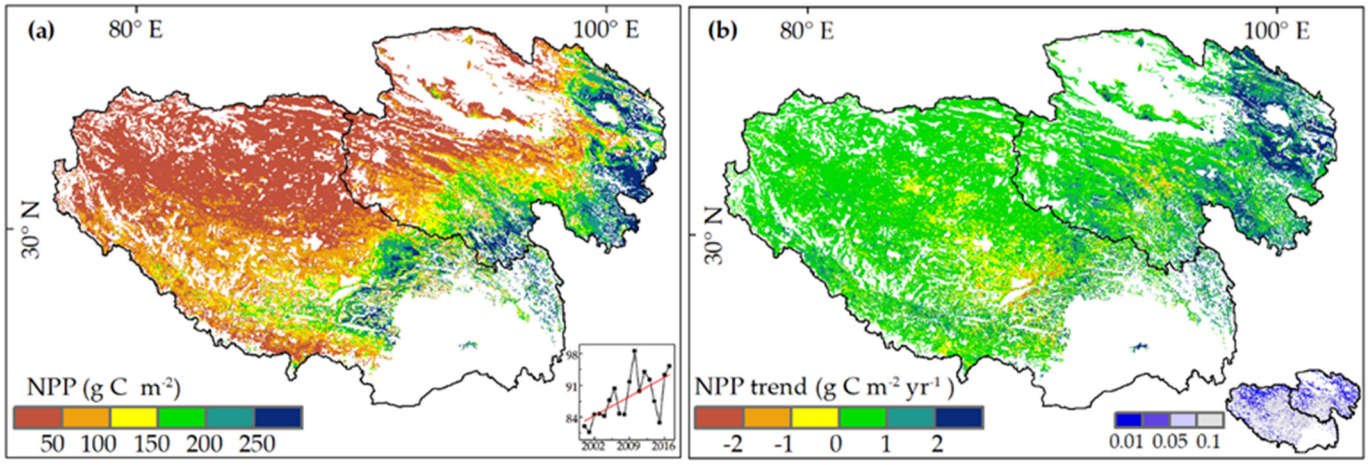

Figure 3. The spatiotemporal patterns of the grassland NPP on the QTP. (**a**) The mean of grassland NPP. The small map at the bottom shows the grassland NPP dynamics from 2000 to 2017. (**b**) The distribution of the trend in grassland NPP. The small map at the bottom shows the range of significance levels.

Table 1. Percentages of grasslands with different variation trends in NPP across the whole plateau and within different grassland types from 2000 to 2017. AM, AS, and DS indicate alpine meadow, alpine steppe, and desert steppe, respectively. Different letters (a, b, c) denote significant differences between them ($p < 0.05$).

	Mean of NPP (g C m^{-2})	Trend of NPP (%)			
		Significant Increasing	Insignificant Increasing	Significant Decreasing	Insignificant Decreasing
AM	133.6 ± 81.5 a	24.63	60.59	0.60	14.17
AS	50.7 ± 50.76 b	36.43	51.57	0.79	11.21
DS	45.1 ± 46.2 c	45.36	50.03	0.21	4.40
total	88.5 ± 78.4	31.34	55.65	0.68	12.33

3.3. Spatiotemporal Patterns of PUE

The grassland PUE showed an evident spatial pattern across the QTP (Figure 4a). The highest PUE were observed in the eastern and western plateau, with values higher than 0.5 g C m^{-2} mm^{-1}, and the central plateau had the lowest PUE (<0.1 g C m^{-2} mm^{-1}). From 2000 to 2017, the annual mean PUE was about 0.25 g C m^{-2} mm^{-1}; the lowest value was 0.21 g C m^{-2} mm^{-1} in 2008 and the highest value was 0.28 g C m^{-2} mm^{-1} in 2009 (Table 2). At the grassland type level, the PUE of alpine steppe (0.19 g C m^{-2} mm^{-1}) was significantly lower than those of alpine meadow (0.31 g C m^{-2} mm^{-1}) and desert steppe (0.32 g C m^{-2} mm^{-1}) (Table 2).

There was no significant change in the PUE during 2000–2017 (Figure 4b). PUE significantly increased and decreased only in 2.96% and 1.59% of grasslands. Within different grassland types, 3.36% of alpine steppe showed a significant increasing trend, and 2.50% of alpine meadow showed a significant decreasing trend in PUE (Table 2).

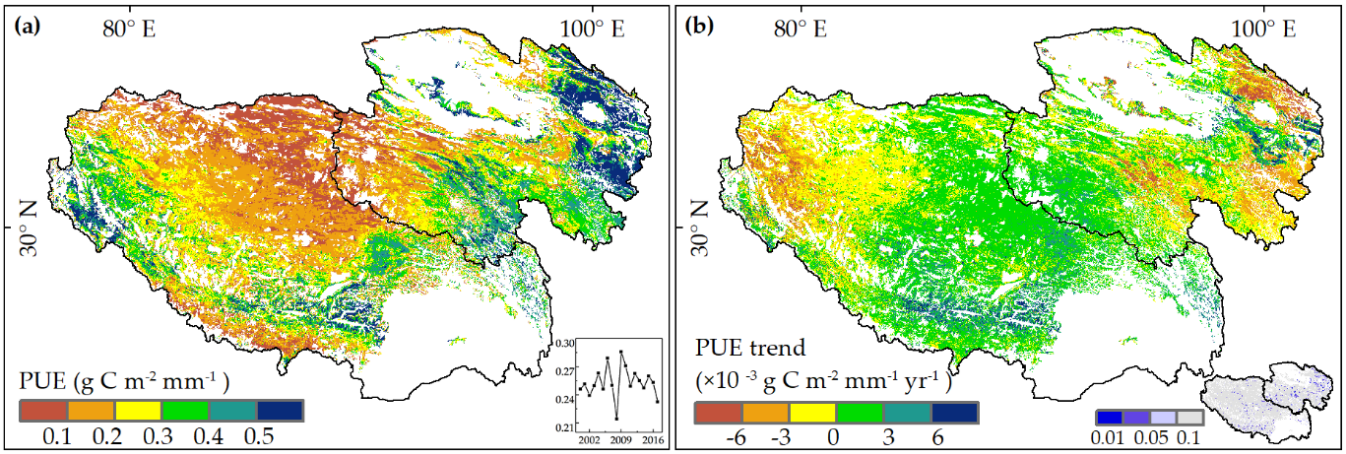

Figure 4. The spatiotemporal patterns of the PUE on the QTP. (**a**) The mean of PUE. The small map at the bottom is the dynamics of the PUE from 2000 to 2017. (**b**) The distribution of the trend in PUE. The small map at the bottom is the range of significance levels.

Table 2. Percentages of grasslands with different variation trends in PUE across the whole plateau and within different grassland types from 2000 to 2017. AM, AS, and DS indicate alpine meadow, alpine steppe, and desert steppe, respectively. Different letters (a, b) denote significant differences between them ($p < 0.05$).

	Mean of PUE (g C m^{-2} mm^{-1})	Trend of PUE (%)			
		Significant Increasing	Insignificant Increasing	Significant Decreasing	Insignificant Decreasing
AM	0.31 ± 0.15 a	2.55	55.33	2.50	39.62
AS	0.19 ± 0.14 b	3.36	53.35	0.86	42.43
DS	0.32 ± 0.15 a	2.32	25.80	0.38	71.51
total	0.25 ± 0.17	2.96	53.31	1.59	42.15

3.4. Relationships of NPP and PUE with Climatic Factors and Grazing Intensity

Figure 5 displays the correlation coefficients of MAT, MAP, and GI with grassland NPP and PUE during 2000–2017. NPP was positively correlated with MAT ($R_{NPP\_MAT} = 0.33$) and MAP ($R_{NPP\_MAP} = 0.32$) but negatively correlated with GI ($R_{NPP\_GI} = -0.06$). Statistical analysis showed that 36.1% and 34.6% of grasslands showed positive and significant ($p < 0.05$) R_{NPP_MAT} and R_{NPP_MAP}, respectively.

The PUE had a weak correlation with MAT ($R_{PUE\_MAT} = 0.2$) and GI ($R_{PUE\_GI} = 0.09$) but a strong correlation with MAP ($R_{PUE\_MAP} = -0.71$). From the space, R_{PUE_MAT} was significant at levels below 0.05 in the southeastern QTP, and R_{PUE_MAT} was significant in almost the entire plateau. The grasslands with significant R_{PUE_MAT} and R_{PUE_GI} only occupied 15.6% and 4.6% of grasslands. However, PUE in over 88% of grasslands had a negative and significant correlation with MAP.

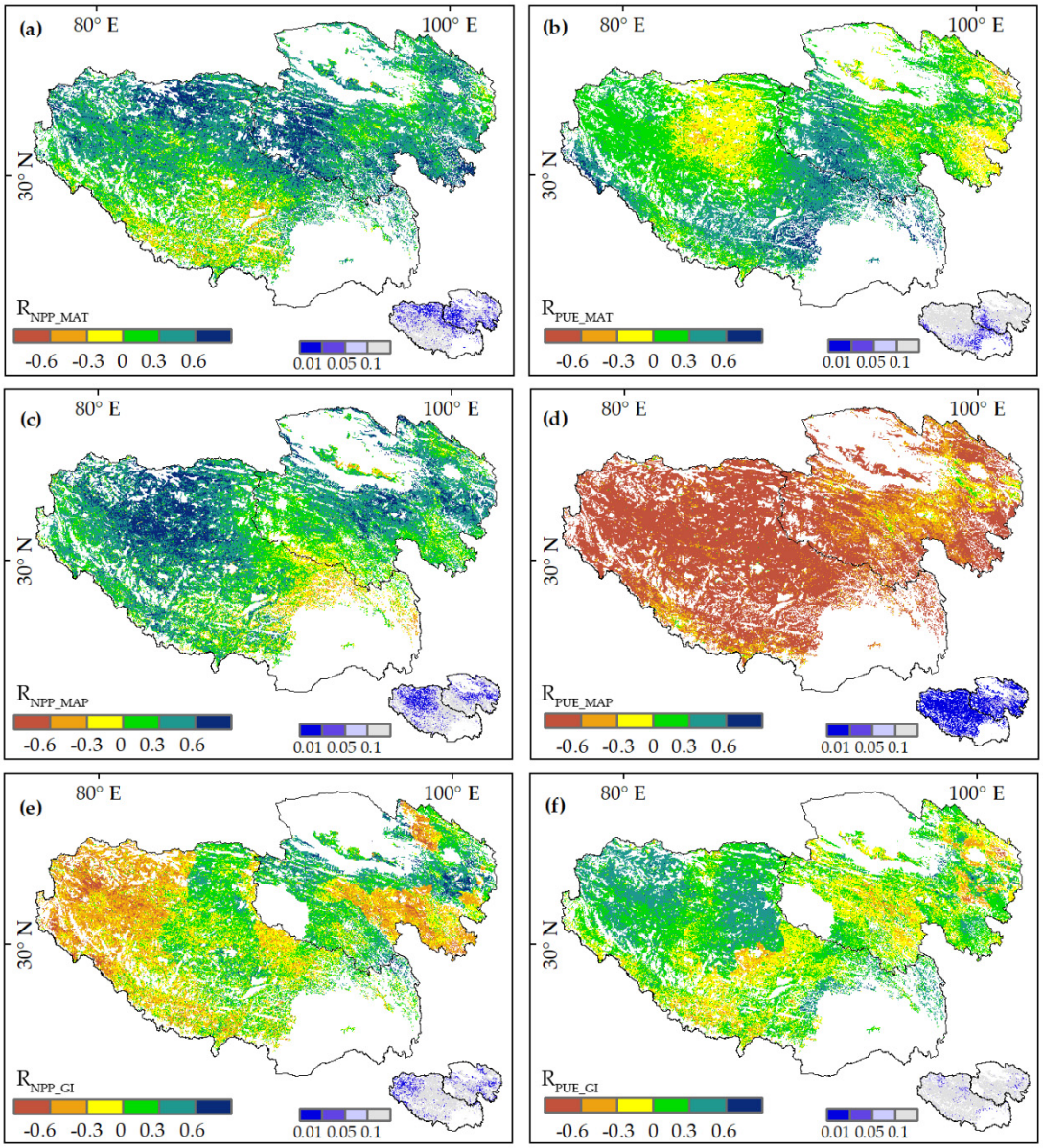

Figure 5. The correlation coefficients of MAT, MAP, and GI with grassland NPP (**a**,**c**,**e**) and PUE (**b**,**d**,**f**) during 2000–2017. Small maps at the bottom are the ranges of significance levels.

3.5. Relative Contributions of Climatic Factors and Grazing Intensity

On the entire QTP, MAT, MAP, and GI explained 17.5%, 14.8%, and 5.5% of NPP variance, respectively. MAT explained more NPP variance than that of MAP in alpine meadow. However, in alpine steppe and desert steppe, MAP explained most of the NPP variance (Table 3). From a spatial perspective, the C_{MAT_NPP} was highest in the northern plateau and lowest in the southwest (Figure 6a). The C_{MAP_NPP} in the southwestern and northeastern parts of the plateau were higher than in other regions (Figure 6b). The C_{GI_NPP} was generally lower than 10% in most areas of the QTP (Figure 6c). Overall, climatic factors dominated the interannual variation of NPP on the QTP (Figure 6d). Statistically, the percentage of MAT-dominated grasslands was the highest (48.9%), followed by MAP-dominated (40%), and the lowest was GI-dominated (11.1%).

In terms of the contributions of MAT, MAP, and GI to PUE interannual variation (C_{MAT_PUE}, C_{MAP_PUE}, C_{GI_PUE}), we found that the C_{MAP_PUE} (52.7%) was significantly higher than C_{MAT_PUE} (9.6%) and C_{GI_PUE} (3.1%) (Figure 7a–c, Table 4). Overall, the per-

centage of MAP-dominated grasslands was 87.9%, and MAT-dominated and GI-dominated areas were 8.8% and 3.3%, respectively (Figure 7d).

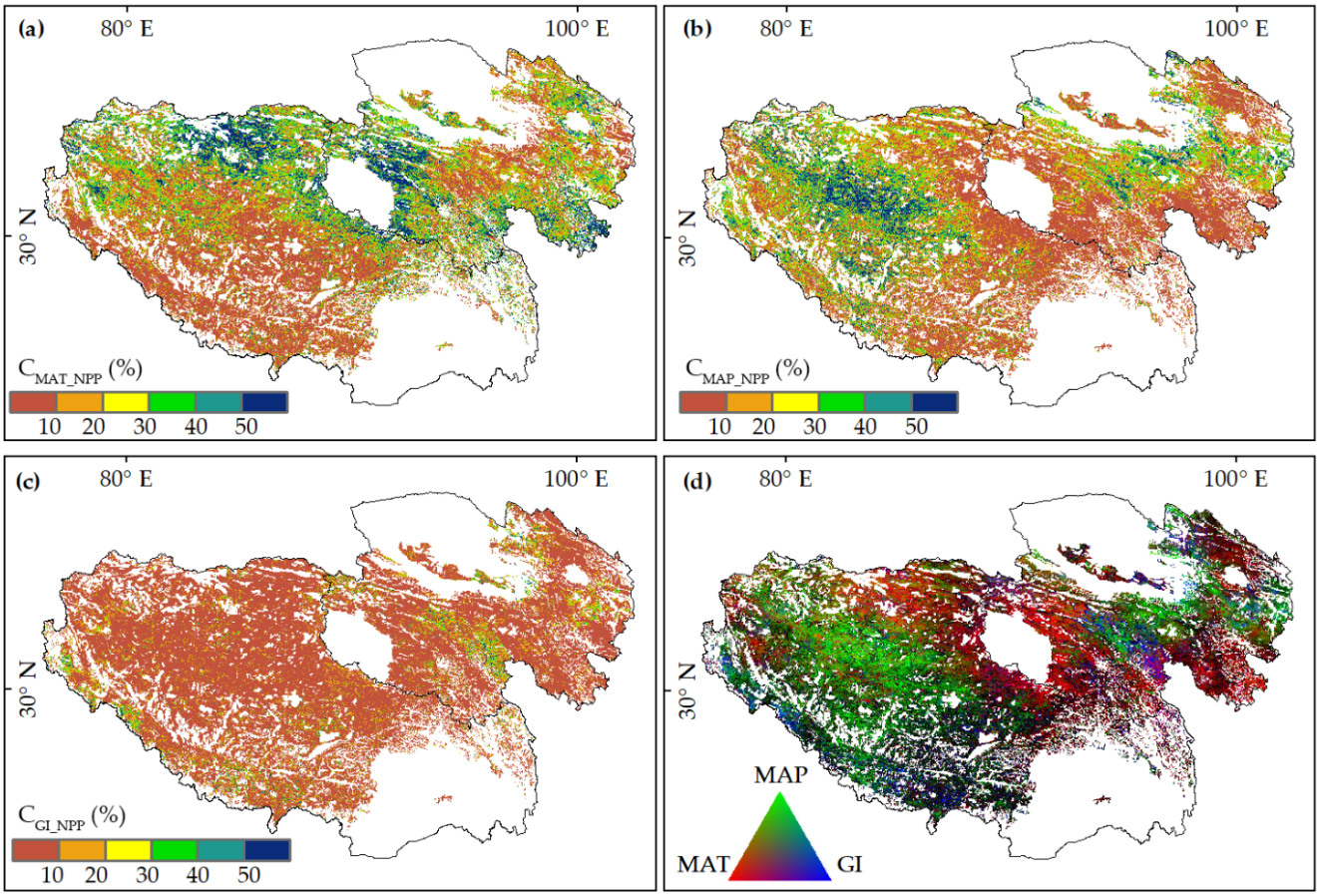

Figure 6. Relative contributions of (**a**) MAT, (**b**) MAP, and (**c**) GI to the NPP interannual variation estimated by generalized linear models (GLMs). (**d**) Spatial pattern of the dominant variables, which was displayed by RGB composite (MAT: red; MAP: green; and GI: blue).

Table 3. Means (±SE) of the relative contributions (%) of mean annual temperature (C_{MAT_NPP}), mean annual precipitation (C_{MAP_NPP}), and grazing intensity (C_{GI_NPP}) to NPP variation estimated by generalized linear model (GLM) across the entire QTP and within alpine meadow (AM), alpine steppe (AS), and desert steppe (DS).

	QTP	AM	AS	DS
C_{MAT_NPP}	17.5 ± 0.01	16.7 ± 0.02	18.3 ± 0.02	16.3 ± 0.07
C_{MAP_NPP}	14.8 ± 0.01	10.3 ± 0.02	18.5 ± 0.02	20.8 ± 0.07
C_{GI_NPP}	5.5 ± 0.01	5.7 ± 0.01	5.1 ± 0.01	6.8 ± 0.04

Table 4. Means (±SE) of the relative contributions (%) of mean annual temperature (C_{MAT_PUE}), mean annual precipitation (C_{MAP_PUE}), and grazing intensity (C_{GI_PUE}) to PUE variation estimated by the generalized linear model (GLM) across the entire QTP and within alpine meadow (AM), alpine steppe (AS), and desert steppe (DS).

	QTP	AM	AS	DS
C_{MAT_PUE}	9.6 ± 0.01	13.3 ± 0.02	6.6 ± 0.01	9.6 ± 0.05
C_{MAP_PUE}	52.7 ± 0.02	45.1 ± 0.03	59.8 ± 0.03	56.4 ± 0.11
C_{GI_PUE}	3.1 ± 0.01	3.5 ± 0.01	3.0 ± 0.01	2.7 ± 0.03

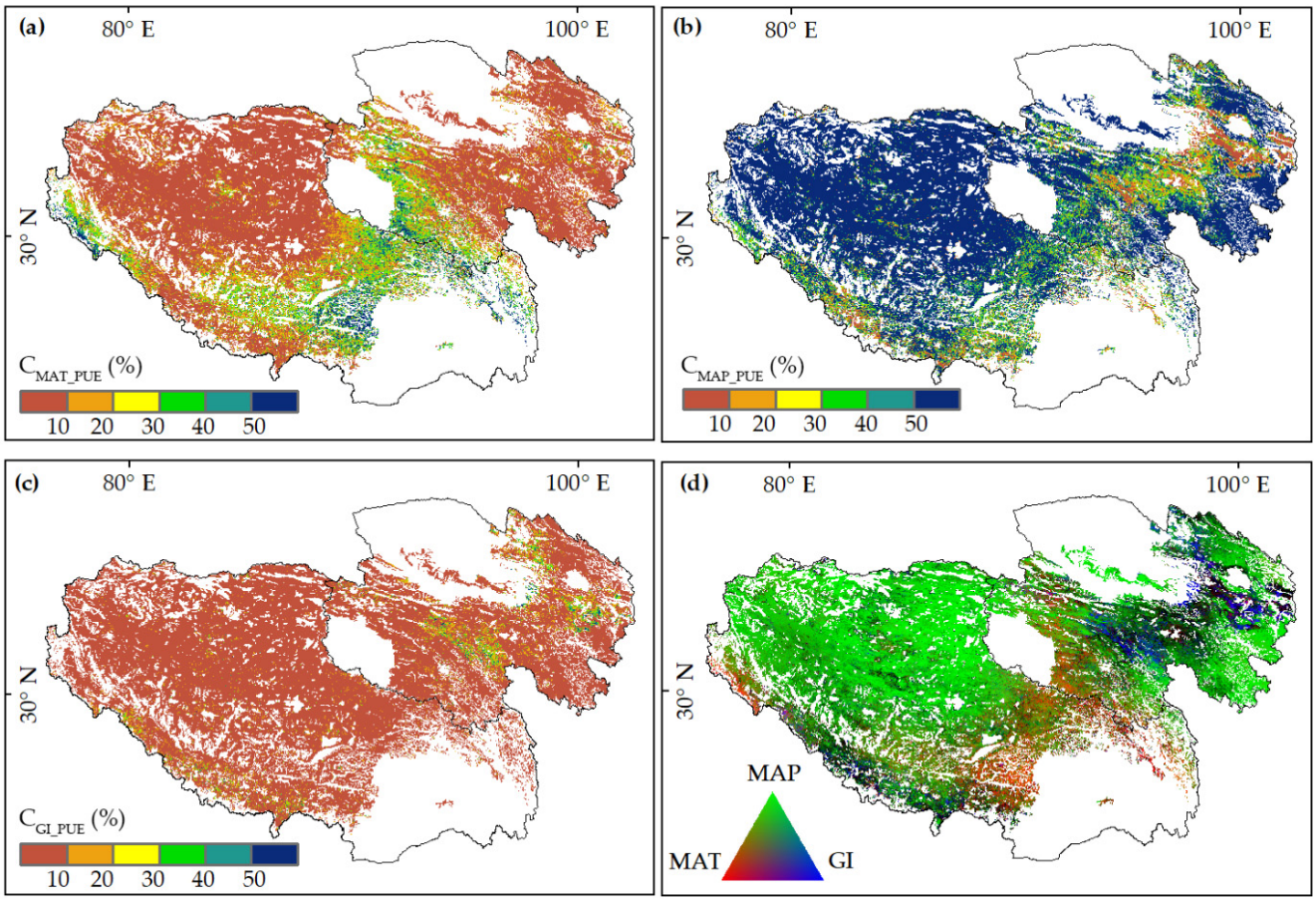

Figure 7. Relative contributions of (**a**) MAT, (**b**) MAP, and (**c**) GI to the PUE interannual variation. (**d**) The spatial pattern of the dominant variables, which was displayed by RGB composite (MAT: red; MAP: green; and GI: blue).

4. Discussion

4.1. Warmer and Wetter Climate Promotes NPP Increases on the QTP

From 2000 to 2017, grassland NPP on the QTP significantly increased at a rate of 0.6 g C m^{-2} $year^{-1}$, with 31.3% and 0.68% of the total grasslands showing significant increasing and decreasing trend, respectively. Spatially, grasslands with increased NPP were mainly distributed in the north of the QTP, and grasslands with decreased NPP were concentrated in the central plateau. The increasing trend in grassland productivity after 2000 had been widely documented by previous studies. For example, Chen et al. [29] found that the mean grassland NPP of the Tibetan Plateau slightly increased from 2000 to 2011. Liu et al. [55] also suggested that the grassland aboveground biomass increased in 70% of the grasslands on the QTP during 2000–2012, mainly concentrated in Qinghai Province. The increases in NPP can be attributed to warmer and wetter climate conditions and decreased grazing intensity. First, the MAT and MAP on the QTP increased with a rate of 0.05 °C/year and 1.8 mm/year from 2000 to 2017, respectively. The warming temperature increases the photosynthesis rate before the vegetation reaches its optimum temperature [56,57]. As water-limited grasslands are greatly sensitive to precipitation, the increased precipitation could stimulate NPP by providing a sufficient water supply, which has been demonstrated by in situ monitoring, satellite monitoring, and manipulative experiments on the QTP [58,59]. Second, the ecological protection projects on the QTP also positively affect grassland productivity [60]. Some conservation efforts, such as fencing grasslands and reducing livestock numbers, have gradually recovered degraded grasslands and promoted grassland productivity [29]. Especially after 2009, the grazing intensity

showed a significant declining trend, causing a noticeable reduction of human-consumed NPP [61].

Given the spatial differentiation of climate change and grazing intensity, the dominant factor for the NPP interannual variation was spatially heterogeneous. On the one hand, climate factors overwhelmed grazing to control grassland NPP dynamics in most of the QTP's grassland areas. A similar finding was made by Lehnert et al. [30], who suggested that although grazing activities could exacerbate the negative effects of the global change, climate factors were still dominant for NPP changes on the QTP. Li et al. [34] also found that the impact of climate change on grasslands NPP was more significant than that of grazing activities. This was possibly caused by the lower intensity of human activity on the QTP than on the rest of the world, due to its vast and sparsely populated environment [4,62]. Since 2000, to protect the ecological environment of this plateau, the Chinese government had launched various policies, such as limiting grazing and fencing degraded grasslands, which have further alleviated the human disturbances on natural grasslands [52]. On the other hand, temperature-dominated and precipitation-dominated grasslands showed a clear spatial pattern. The temperature was the limiting factor in mid-eastern QTP. Precipitation dominated the grassland changes in the southwestern and northeastern parts of the plateau. This spatial pattern was similar to the findings in Li et al. [63] and Huang et al. [64], showing that the mid-eastern grasslands were more sensitive to temperature, and the southwestern and northeastern grasslands were more sensitive to precipitation. The spatially varied limiting factors were closely correlated with the complex meteorological and biotic conditions of the QTP [65]. In arid and semi-arid regions such as the alpine steppe in northern Tibet, vegetation can quickly respond to precipitation. However, in humid areas such as alpine meadow in southern Qinghai, the temperature became prominent due to adequate moisture [63,66].

4.2. The Spatiotemporal Variation of PUE

The averaged PUE of the alpine grasslands, over 2000–2017, was 0.25 g C m^{-2} mm^{-1}, which is within the range of global grasslands (0.05–1.81 g m^{-2} mm^{-1}) reported by Le Houérou H.N et al. [67] and within the range of China's grasslands (0.13–0.64 g m^{-2} mm^{-1}) reported by Hu et al. [15]. Further, it was found in this study that the QTP's PUE was grassland type-dependent. Alpine steppe's PUE (0.19 g C m^{-2} mm^{-1}) was significantly lower than those of alpine meadow (0.31 g C m^{-2} mm^{-1}) and desert steppe (0.32 g C m^{-2} mm^{-1}). This may be caused by vegetation composition and environmental conditions. For example, the high species richness can respond to high precipitation and use the available water completely [31,68], leading to a larger PUE in the alpine meadow. The soil texture is another factor that affects the PUE of alpine grassland by altering the soil water retention. The high silt content and low sand content in alpine meadows generally cause a high water-holding capacity, which is conducive to shaping a high PUE [31,69]. However, it should be noted that desert steppe with a low species richness and silt content also had a high PUE. The potential explanation is that plants in desert steppe usually can also absorb deep water to adapt to an extremely dry climate [70]. Plants in arid regions can resist water stress through some trade-offs between functional traits, such as changing the thickness and size of leaves [32,71].

From 2000 to 2017, the grassland's PUE on the QTP showed fluctuations with non-significant interannual variations. Precipitation was significantly and negatively correlated with PUE and contributed to most variations of PUE. These are in line with the findings of previous studies in different regions. For example, Liu and Huang [72] proposed that the PUE of alpine grasslands on the QTP showed a significantly negative correlation with precipitation. Bai et al. [53] suggested that temperate grasslands' PUE in the Inner Mongolian steppe region decreased with increased annual precipitation. Huxman et al. [20] reported that grasslands in North and South America had maximal PUE in the driest years. The underlying mechanisms of PUE interannual variations were involved with the interactions among precipitation, nutrient, and biotic factors [53]. First, long-term

saturated soil moisture is likely to reduce root and soil microbial activity by limiting oxygen supply and then curbing vegetation growth [73]. Second, although increased precipitation alleviates the available water limitations, nitrogen availability limitations may be strengthened to constrain the response of production to increased precipitation, resulting in a lower PUE [53,74]. Finally, the species in arid and semi-arid regions generally have relatively low growth rates to promote their drought-enduring ability, which enables limiting the response of vegetation to extreme drought events [75]. Therefore, the PUE of alpine grasslands in the south of QTP showed an increasing trend despite the MAP decreased across this region.

4.3. The Effects of GI on Vegetation Growth

Compared with MAT and MAP, the GI had the lowest contributions to NPP and PUE variation. However, 11.1% and 3.3% of the grasslands' NPP and PUE were dominated by GI. For grasslands on the QTP, grazing is one of the most typical human disturbances, significantly affecting native species diversity and ecosystem stability [76]. From 2000 to 2017, the GI on this plateau presented "converse-U" changes. The highest GI was generated in 2007 (0.72 SSU/ha) and then declined significantly due to the strict livestock reduction policy. In this period, NPP showed a negative correlation with GI, suggesting that this decrease in GI had a positive effect on vegetation growth. This information about the relationship between grazing activities and vegetation productivity is beneficial to policymakers and herders to develop specific policies and sustainable management strategies. However, the relationship between grazing activities and vegetation growth was complicated due to its complex and diverse processes, such as forage selection and trampling. Numerous studies viewed grazing as detrimental to plant growth [77]. However, the moderate interference hypothesis suggested that moderate grazing intensity may lead to compensatory growth and then positively affect grassland productivity [78,79]. Undoubtedly, overgrazing could, directly and indirectly, destroy the structure and function of grassland ecosystems. Thus, for grasslands where grazing dominates vegetation growth, it is necessary to investigate how grazing intensity affects grassland changes and speculate on the possible underlying mechanisms based on grazing-manipulated experiments.

4.4. Limitations and Uncertainties

This study aimed to reveal the relative contributions of climate factors (precipitation and temperature) and grazing to interannual NPP and PUE variations on the QTP. It should be noted that the effects of land cover changes on the dynamics of NPP and PUE were not considered, although they have modified or amplified the biogeochemical cycling of grassland ecosystems [26]. In the future, to deepen our understanding of the mechanism underlying the climate–vegetation–human relationship, the roles of human-induced land use/cover change in influencing the variations of NPP or PUE should be taken into consideration. Besides, the simulated NPP had some shortcomings; for example, the maximum LUE was treated as a constant for the entire grassland area instead of treating the alpine meadow, alpine steppe, and desert steppe separately. We thus emphasize the need for complementary studies at the local scale with field surveys to calculate the maximum LUE for each grassland type on the QTP. In addition, the CASA model was run using temperature, precipitation, and solar radiation, resulting in the autocorrelations of simulated NPP with climate factors. To quantify the influences of the autocorrelation on the results of GLMs, we further used growing-season NDVI (GSNDVI) as a surrogate of NPP to construct GLMs. We found that the relative contributions of temperature, precipitation, and grazing to GSNDVI were similar to those to NPP (Figure S1), suggesting that the autocorrelations between NPP and climate factors had no significant effects on the conclusions.

5. Conclusions

This study investigated the spatial and temporal patterns of grassland NPP and PUE on the QTP from 2000 to 2017. It was found that the NPP decreased from the southeast to the northwest on this plateau. However, the PUE was higher at the eastern and western ends of the plateau, but was lower in the center. Over time, NPP showed a significant increasing trend, and PUE showed a non-significant increasing trend. The relative contributions of climatic factors (temperature and precipitation) and grazing intensity to the temporal variations of NPP and PUE were quantified by GLMs. Although numerous studies claimed that overgrazing impaired the structure and function of alpine grasslands, our research found climatic factors played a dominant role in vegetation changes on the QTP.

Supplementary Materials: The following are available online at https://www.mdpi.com/article/10.3390/rs13173424/s1, Figure S1: Relative contributions of (a) MAT, (b) MAP, and (c) GI to the growing-season NDVI (GSNDVI) interannual variation estimated by generalized linear models (GLMs). (d) Spatial pattern of the dominant variables, which was displayed by RGB composite (MAT: red; MAP: green; and GI: blue).

Author Contributions: M.L. conceptualized this study. M.L. and H.Y. collected and analyzed the data. H.Y. led the writing. Q.D., B.M., Y.L., C.L., X.Z., Y.S. and S.Y. interpreted the results and revised the text. All authors have read and agreed to the published version of the manuscript.

Funding: The study was supported by the National Key R&D Program of China (2017YFA0604801) and the National Nature Science Foundation of China (31901393).

Institutional Review Board Statement: Not applicable.

Informed Consent Statement: Not applicable.

Data Availability Statement: The monthly MOD13A3C6 NDVI data were obtained from the NASA LP DAAC (Land Processes Distributed Active Archive Center) website (https://lpdaac.usgs.gov/get_data/data_pool, accessed on 1 May 2020). The meteorological data were downloaded from the National Meteorological Information Center of China Meteorological Administration (http://geodata.cn, accessed on 1 May 2020). Grassland distribution was determined by the China Vegetation Atlas with a scale of 1:1,000,000, which was derived from the Resource and Environment Data Cloud Platform (http://www.resdc.cn/data.aspx?DATAID=122, accessed on 1 May 2020).

Acknowledgments: We are very grateful to the Three-River-Source National Park Administration for their support of our field survey. We sincerely appreciate the editor and three anonymous reviewers for their constructive comments and suggestions. We acknowledge the support of all co-authors for their constructive and helpful comments and organization of this study.

Conflicts of Interest: The authors declare that the research was conducted in the absence of any commercial or financial relationships that could be construed as a potential conflict of interest.

References

1. Radu, D.D.; Duval, T.P. Precipitation Frequency Alters Peatland Ecosystem Structure and CO_2 Exchange: Contrasting Effects on Moss, Sedge, and Shrub Communities. *Glob. Chang. Biol.* **2018**, *24*, 2051–2065. [CrossRef]
2. DeFries, R. Past and Future Sensitivity of Primary Production to Human Modification of the Landscape. *Geophys. Res. Lett.* **2002**, *29*, 36-1–36-4. [CrossRef]
3. Vitousek, P.M.; Mooney, H.A.; Lubchenco, J.; Melillo, J.M. Human Domination of Earth's Ecosystems. *Science* **1997**, *277*, 494–499. [CrossRef]
4. Venter, O.; Sanderson, E.W.; Magrach, A.; Allan, J.R.; Beher, J.; Jones, K.R.; Possingham, H.P.; Laurance, W.F.; Wood, P.; Fekete, B.M. Sixteen Years of Change in the Global Terrestrial Human Footprint and Implications for Biodiversity Conservation. *Nat. Commun.* **2016**, *7*, 12558. [CrossRef] [PubMed]
5. Seiferling, I.; Proulx, R.; Wirth, C. Disentangling the Environmental-Heterogeneity Species-Diversity Relationship Along a Gradient of Human Footprint. *Ecology* **2014**, *95*, 2084–2095. [CrossRef] [PubMed]
6. Piao, S.; Wang, X.; Park, T.; Chen, C.; Lian, X.; He, Y.; Bjerke, J.W.; Chen, A.; Ciais, P.; Tømmervik, H.; et al. Characteristics, Drivers and Feedbacks of Global Greening. *Nat. Rev. Earth Environ.* **2020**, *1*, 14–27. [CrossRef]
7. Gil, M.A.; Baskett, M.L.; Munch, S.B.; Hein, A.M. Fast Behavioral Feedbacks Make Ecosystems Sensitive to Pace and Not Just Magnitude of Anthropogenic Environmental Change. *Proc. Natl. Acad. Sci. USA* **2020**, *117*, 25580–25589. [CrossRef]

8. Chen, T.; Bao, A.M.; Jiapaer, G.; Guo, H.; Zheng, G.X.; Jiang, L.L.; Chang, C.; Tuerhanjiang, L. Disentangling the Relative Impacts of Climate Change and Human Activities on Arid and Semi-Arid Grasslands in Central Asia during 1982–2015. *Sci. Total Environ.* **2019**, *653*, 1311–1325. [CrossRef]
9. Curlock, J.M.O.S.; Hall, D.O. The Global Carbon Sink: A Grassland Perspective. *Glob. Chang. Biol.* **2010**, *4*, 229–233. [CrossRef]
10. Xie, G.D.; Zhang, Y.L.; Lu, C.X. Study on Valuation of Rangeland Ecosystem Services of China. *J. Natl. Resour.* **2001**, *16*, 47–53.
11. Gang, C.; Zhou, W.; Chen, Y.; Wang, Z.; Sun, Z.; Li, J.; Qi, J.; Odeh, I. Quantitative Assessment of the Contributions of Climate Change and Human Activities on Global Grassland Degradation. *Environ. Earth Sci.* **2014**, *72*, 4273–4282. [CrossRef]
12. Gao, Y.; Zhou, X.; Wang, Q.; Wang, C.; Zhan, Z.; Chen, L.; Yan, J.; Qu, R. Vegetation Net Primary Productivity and Its Response to Climate Change During 2001–2008 in the Tibetan Plateau. *Sci. Total Environ.* **2013**, *444*, 356–362. [CrossRef]
13. Nemani, R.R.; Keeling, C.D.; Hashimoto, H.; Jolly, W.M.; Piper, S.C.; Tucker, C.J.; Myneni, R.B.; Running, S.W. Climate-Driven Increases in Global Terrestrial Net Primary Production from 1982 to 1999. *Science* **2003**, *300*, 1560–1563. [CrossRef] [PubMed]
14. Ling, L.; Xin, L.; Huang, C.L.; Veroustraete, F. Analysis of the Spatio-Temporal Characteristics of Water Use Efficiency of Vegetation in West China. *J. Glaciol. Geocryol.* **2007**, *29*, 777–784.
15. Hu, Z.; Yu, G.; Fan, J.; Zhong, H.; Wang, S.; Li, S. Precipitation-Use Efficiency Along a 4500-km Grassland Transect. *Glob. Ecol. Biogeogr.* **2010**, *19*, 842–851.
16. Siepielski, A.M.; Morrissey, M.B.; Buoro, M.; Carlson, S.M.; Caruso, C.M.; Clegg, S.M.; Coulson, T.; DiBattista, J.; Gotanda, K.M.; Francis, C.D.; et al. Precipitation Drives Global Variation in Natural Selection. *Science* **2017**, *355*, 959–962. [CrossRef]
17. Knapp, A.K.; Fay, P.A.; Blair, J.M.; Collins, S.L.; Smith, M.D.; Carlisle, J.D.; Harper, C.W.; Danner, B.T.; Lett, M.S.; McCarron, J.K. Rainfall Variability, Carbon Cycling, and Plant Species Diversity in a Mesic Grassland. *Science* **2002**, *298*, 2202–2205. [CrossRef] [PubMed]
18. Wang, S.; Zhang, B.; Yang, Q.; Chen, G.; Yang, B.; Lu, L.; Shen, M.; Peng, Y. Responses of Net Primary Productivity to Phenological Dynamics in the Tibetan Plateau, China. *Agric. For. Meteorol.* **2017**, *232*, 235–246. [CrossRef]
19. Piao, S.; Friedlingstein, P.; Ciais, P.; Viovy, N.; Demarty, J. Growing Season Extension and Its Impact on Terrestrial Carbon Cycle in the Northern Hemisphere Over the Past 2 Decades. *Glob. Biogeochem. Cycles* **2007**, *21*, 116–123. [CrossRef]
20. Huxman, T.E.; Smith, M.D.; Fay, P.A.; Knapp, A.K.; Shaw, M.R.; Loik, M.E.; Smith, S.D.; Tissue, D.T.; Zak, J.C.; Weltzin, J.F.; et al. Convergence Across Biomes to a Common Rain-Use Efficiency. *Nature* **2004**, *429*, 651–654. [CrossRef]
21. Rockström, J.; Steffen, W.; Noone, K.; Persson, Å.; Chapin, F.S.; Lambin, E.F.; Lenton, T.M.; Scheffer, M.; Folke, C.; Schellnhuber, H.J.; et al. Safe Operating Space for Humanity. *Nature* **2009**, *461*, 472–475. [CrossRef] [PubMed]
22. Niu, Y.; Zhu, H.; Yang, S.; Ma, S.; Zhou, J.; Chu, B.; Hua, R.; Hua, L. Overgrazing Leads to Soil Cracking That Later Triggers the Severe Degradation of Alpine Meadows on the Tibetan Plateau. *Land Degrad. Dev.* **2019**, *30*, 1243–1257. [CrossRef]
23. Han, Q.; Luo, G.; Li, C.; Xu, W. Modeling the Grazing Effect on Dry Grassland Carbon Cycling with Biome-BGC Model. *Ecol. Complex.* **2014**, *17*, 149–157. [CrossRef]
24. Wang, C.S.; Meng, F.D.; Li, X.E.; Jiang, L.L.; Wang, S.P. Responses of Alpine Grassland Ecosystem on Tibetan Plateau to Climate Change: A Mini Review. *Chin. J. Ecol.* **2013**, *32*, 1587–1595.
25. Yao, T.; Wu, F.; Ding, L.; Sun, J.; Zhu, L.; Piao, S.; Deng, T.; Ni, X.; Zheng, H.; Ouyang, H. Multispherical Interactions and Their Effects on the Tibetan Plateau's Earth System: A Review of the Recent Researches. *Natl. Sci. Rev.* **2015**, *2*, 468–488. [CrossRef]
26. Chen, H.; Zhu, Q.; Peng, C.; Wu, N.; Wang, Y.; Fang, X.; Gao, Y.; Zhu, D.; Yang, G.; Tian, J.; et al. The Impacts of Climate Change and Human Activities on Biogeochemical Cycles on the Qinghai-Tibetan Plateau. *Glob. Chang. Biol.* **2013**, *19*, 2940–2955. [CrossRef]
27. Fan, J.; Yong, X.U.; Wang, C.S.; Niu, Y.F.; Chen, D.; Sun, W. The Effects of Human Activities on the Ecological Environment of Tibet Over the Past Half Century. *Chin. Sci. Bull.* **2015**, *60*, 3057–3066. [CrossRef]
28. Dong, S.K.; Li, J.P.; Li, X.Y.; Wen, L.; Zhu, L.; Li, Y.Y.; Ma, Y.S.; Shi, J.J.; Dong, Q.M.; Wang, Y.L. Application of Design Theory for Restoring the "Black Beach" Degraded Rangeland at the Headwater Areas of the Qinghai-Tibetan Plateau. *Afr. J. Agric. Res.* **2010**, *5*, 3542–3552.
29. Chen, B.; Zhang, X.; Tao, J.; Wu, J.; Wang, J.; Shi, P.; Zhang, Y.; Yu, C. The Impact of Climate Change and Anthropogenic Activities on Alpine Grassland Over the Qinghai-Tibet Plateau. *Agric. For. Meteorol.* **2014**, *189*, 11–18. [CrossRef]
30. Lehnert, L.W.; Wesche, K.; Trachte, K.; Reudenbach, C.; Bendix, J. Climate Variability Rather Than Overstocking Causes Recent Large Scale Cover Changes of Tibetan Pastures. *Sci. Rep.* **2016**, *6*, 24367. [CrossRef]
31. Yang, Y.H.; Fang, J.Y.; Fay, P.A.; Bell, J.E.; Ji, C.J. Rain Use Efficiency Across a Precipitation Gradient on the Tibetan Plateau. *Geophys. Res. Lett.* **2010**, *37*. [CrossRef]
32. Zhao, G.; Liu, M.; Shi, P.; Zong, N.; Wang, J.; Wu, J.; Zhang, X. Spatial–Temporal Variation of ANPP and Rain-Use Efficiency Along a Precipitation Gradient on Changtang Plateau, Tibet. *Remote Sens.* **2019**, *11*, 325. [CrossRef]
33. Sun, H.; Zheng, D.; Yao, T.; Zhang, Y. Protection and Construction of the National Ecological Security Shelter Zone on Tibetan Plateau. *Acta Geogr. Sin.* **2012**, *67*, 3–12.
34. Li, M.; Wu, J.S.; Feng, Y.F.; Niu, B.; He, Y.T.; Zhang, X.Z. Climate Variability Rather Than Livestock Grazing Dominates Changes in Alpine Grassland Productivity Across Tibet. *Front. Ecol. Evol.* **2021**, *9*. [CrossRef]
35. Long, R.J.; Apori, S.O.; Castro, F.B.; Orskov, E.R. Feed Value of Native Forages of the Tibetan Plateau of China. *Anim. Feed Sci. Tech.* **1999**, *80*, 101–113. [CrossRef]
36. Mirjanka, L.; Brankica, M. Albers Conical Equal-Area Projection. *Geod. List* **1996**, *2*, 161–170.

37. Jonsson, P.; Eklundh, L. TIMESAT-A Program for Analyzing Time-Series of Satellite Sensor Data. *Comput. Geosci.-UK* **2004**, *30*, 833–845. [CrossRef]
38. Eklundh, L.; Jönsson, P. TIMESAT: A Software Package for Time-Series Processing and Assessment of Vegetation Dynamics. In *Remote Sensing Time Series*; Springer: Cham, Switzerland, 2015.
39. Luo, J.; Ying, K.; Bai, J. Savitzky–Golay Smoothing and Differentiation Filter for Even Number Data. *Signal. Process.* **2005**, *85*, 1429–1434. [CrossRef]
40. Allan, R.; Pereira, L.; Smith, M. *Crop. Evapotranspiration-Guidelines for Computing Crop Water Requirements*; FAO: Rome, Italy, 1998.
41. Hutchinson, M. *Anusplin Version 4.3. Centre for Resource and Environmental Studies*; Australian National University: Canberra, Australia, 2004.
42. Cao, Y.; Wu, J.; Zhang, X.; Niu, B.; He, Y. Comparison of Methods for Evaluating the Forage-Livestock Balance of Alpine Grasslands on the Northern Tibetan Plateau. *J. Resour. Ecol.* **2020**, *11*, 272–282.
43. Monteith, J.L.; Moss, C.J.; Cooke, G.W.; Pirie, N.W.; Bell, G.D.H. Climate and the Efficiency of Crop Production in Britain. *Philos. Trans. R. Soc. London B Biol. Sci.* **1977**, *281*, 277–294.
44. Potter, C.S.; Randerson, J.T.; Field, C.B.; Matson, P.A.; Vitousek, P.M.; Mooney, H.A.; Klooster, S.A. Terrestrial Ecosystem Production: A Process Model Based on Global Satellite and Surface Data. *Glob. Biogeochem. Cycles* **1993**, *7*, 811–841. [CrossRef]
45. Potter, C. Predicting Climate Change Effects on Vegetation, Soil Thermal Dynamics, and Carbon Cycling in Ecosystems of Interior Alaska. *Ecol. Model.* **2004**, *175*, 1–24. [CrossRef]
46. Piao, S.; Fang, J.; He, J. Variations in Vegetation Net Primary Production in the Qinghai-Xizang Plateau, China, from 1982 to 1999. *Clim. Chang.* **2006**, *74*, 253–267. [CrossRef]
47. Yuan, J.; Niu, Z.; Wang, C. Vegetation NPP Distribution Based on MODIS Data and CASA Model-A Case Study of Northern Hebei Province. *Chin. Geogr. Sci.* **2006**, *16*, 334–341. [CrossRef]
48. Field, C.B.; Randerson, J.T.; Malmström, C.M. Global Net Primary Production: Combining Ecology and Remote Sensing. *Remote Sens. Environ.* **1995**, *51*, 74–88. [CrossRef]
49. Field, C.B.; Behrenfeld, M.J.; Randerson, J.T.; Falkowski, P. Primary Production of the Biosphere: Integrating Terrestrial and Oceanic Components. *Science* **1998**, *281*, 237–240. [CrossRef] [PubMed]
50. Wang, H.; Jia, G.; Fu, C.; Feng, J.; Zhao, T.; Ma, Z. Deriving Maximal Light Use Efficiency From Coordinated Flux Measurements and Satellite Data for Regional Gross Primary Pro-Duction Modeling. *Remote Sens. Environ.* **2010**, *114*, 2248–2258. [CrossRef]
51. Zhang, Y.; Qi, W.; Zhou, C.; Ding, M.; Liu, L.; Gao, J.; Bai, W.; Wang, Z.; Zheng, D. Spatial and Temporal Variability in the Net Primary Production of Alpine Grassland on the Tibetan Plateau Since 1982. *J. Geogr. Sci.* **2014**, *24*, 269–287. [CrossRef]
52. Li, M.; Zhang, X.; Wu, J.; Ding, Q.; He, Y. Declining Human Activity Intensity on Alpine Grasslands of the Tibetan Plateau. *J. Environ. Manag.* **2021**, *296*, 113198. [CrossRef]
53. Bai, Y.; Wu, J.; Xing, Q.; Pan, Q.; Huang, J.; Yang, D.; Han, X. Primary Production and Rain Use Efficiency Across a Precipitation Gradient on the Mongolia Plateau. *Ecology* **2008**, *89*, 2140–2153. [CrossRef]
54. Zhang, L.X.; Fan, J.W.; Shao, Q.Q.; Tang, F.P.; Zhang, H.Y.; Yu-Zhe, L.I. Changes in Grassland Yield and Grazing Pressure in the Three Rivers Headwater Region Before and After the Implementation of the Eco-Restoration Project. *Acta Pratacult. Sin.* **2014**, *23*, 116–123.
55. Liu, S.; Cheng, F.; Dong, S.; Zhao, H.; Hou, X.; Wu, X. Spatiotemporal Dynamics of Grassland Aboveground Biomass on the Qinghai-Tibet Plateau Based on Validated MODIS NDVI. *Sci. Rep.* **2017**, *7*, 4182. [CrossRef]
56. Zhao, J.; Hartmann, H.; Trumbore, S.; Ziegler, W.; Zhang, Y. High Temperature Causes Negative Whole-Plant Carbon Balance under Mild Drought. *New Phytol.* **2013**, *200*, 330–339. [CrossRef]
57. Hudson, J.; Henry, G.; Cornwell, W.K. Taller and Larger: Shifts in Arctic Tundra Leaf Traits After 16 Years of Experimental Warming. *Glob. Chang. Biol.* **2011**, *17*, 1013–1021. [CrossRef]
58. Qun, G.; Zhongmin, H.; Shenggong, L.; Guirui, Y.; Xiaomin, S.; Leiming, Z.; Songlin, M.; Xianjin, Z.; Yanfen, W.; Yingnian, L.; et al. Contrasting Responses of Gross Primary Productivity to Precipitation Events in a Water-Limited and a Temperature-Limited Grassland Ecosystem. *Agric. For. Meteorol.* **2015**, *214*, 169–177.
59. Fu, G.; Shen, Z.X.; Zhang, X.Z. Increased Precipitation Has Stronger Effects on Plant Production of an Alpine Meadow Than Does Experimental Warming in the Northern Tibetan Plateau. *Agric. For. Meteorol.* **2018**, *249*, 11–21. [CrossRef]
60. Zhang, Q.; Li, M.A.; Zhang, Z.; Wenhua, X.U.; Zhou, B.; Song, M.; Qiao, A.; Wang, F.; She, Y.; Yang, X. Ecological Restoration of Degraded Grassland in Qinghai-Tibet Alpine Region: Degradation Status, Restoration Measures, Effects and Prospects. *Acta Ecol. Sin.* **2019**, *39*, 7441–7451.
61. Zhang, Y.; Pan, Y.; Zhang, X.; Wu, J.; Yu, C.; Li, M.; Wu, J. Patterns and Dynamics of the Human Appropriation of Net Primary Production and Its Components in Tibet. *J. Environ. Manag.* **2018**, *210*, 280–289. [CrossRef]
62. Li, S.; Wu, J.; Jian, G.; Li, S. Human Footprint in Tibet: Assessing the Spatial Layout and Effectiveness of Nature Reserves. *Sci. Total Environ.* **2018**, *621*, 18–29. [CrossRef]
63. Li, L.; Zhang, Y.; Liu, L.; Wu, J.; Wang, Z.; Li, S.; Zhang, H.; Zu, J.; Ding, M.; Paudel, B. Spatiotemporal Patterns of Vegetation Greenness Change and Associated Climatic and Anthropogenic Drivers on the Tibetan Plateau during 2000–2015. *Remote Sens.* **2018**, *10*, 1525. [CrossRef]
64. Huang, K.; Zhang, Y.; Zhu, J.; Liu, Y.; Zu, J.; Zhang, J. The Influences of Climate Change and Human Activities on Vegetation Dynamics in the Qinghai-Tibet Plateau. *Remote Sens.* **2016**, *8*, 876. [CrossRef]

65. Molnar, P.; Boos, W.; Battisti, D. Orographic Controls on Climate and Paleoclimate of Asia: Thermal and Mechanical Roles for the Tibetan Plateau. *Annu. Rev. Earth Planet. Sci.* **2010**, *38*, 77–102. [CrossRef]
66. Xu, X.; Chen, H.; Levy, J.K. Spatiotemporal Vegetation Cover Variations in the Qinghai-Tibet Plateau under Global Climate Change. *Chin. Sci. Bull.* **2008**, *53*, 915–922. [CrossRef]
67. Le Houérou, H.N.; Bingham, R.L.; Skerbek, W. Relationship Between the Variability of Primary Production and the Variability of Annual Precipitation in World Arid Lands. *J. Arid Environ.* **1988**, *15*, 1–18. [CrossRef]
68. Paruelo, J.M.; Lauenroth, W.K.; Burke, I.C.; Sala, O.E. Grassland Precipitation-Use Efficiency Varies Across a Resource Gradient. *Ecosystems* **1999**, *2*, 64–68. [CrossRef]
69. Epstein, H.E.; Lauenroth, W.K.; Burke, I.C. Effects of Temperature and Soil Texture on ANPP in the U.S. Great Plants. *Ecology* **1997**, *78*, 2628–2631. [CrossRef]
70. Jobbágy, E.; Sala, O. Controls of Grass and Shrub Aboveground Production in the Patagonian Steppe. *Ecol. Appl.* **2000**, *10*, 541–549. [CrossRef]
71. Wei, H.; Wu, B.; Yang, W.; Luo, T. Low Rainfall-Induced Shift in Leaf Trait Relationship within Species Along a Semi-Arid Sandy Land Transect in Northern China. *Plant Biol.* **2011**, *13*, 85–92. [CrossRef]
72. Liu, Z.; Huang, M. Assessing Spatio-Temporal Variations of Precipitation-Use Efficiency Over Tibetan Grasslands Using MODIS and In-Situ Obser-Vations. *Front. Earth Sci.* **2016**, *10*, 784–793. [CrossRef]
73. Shi, S.B. The Photosynthesis of Plant Community in Kobresia humilis Meadow. *Chin. J. Plant Ecol.* **1996**, *20*, 225–234.
74. Knapp, A.K.; Smith, M.D. Variation Among Biomes in Temporal Dynamics of Aboveground Primary Production. *Science* **2001**, *291*, 481–484. [CrossRef]
75. Ogaya, R.; Peuelas, J. Comparative Field Study of Quercus ilex and Phillyrea latifolia: Photosynthetic Response to Experimental Drought Conditions. *Environ. Exp. Bot.* **2003**, *50*, 137–148. [CrossRef]
76. Wu, J.; Zhang, X.; Shen, Z.; Shi, P.; Xu, X.; Li, X. Grazing-Exclusion Effects on Aboveground Biomass and Water-Use Efficiency of Alpine Grasslands on the Northern Tibetan Plateau. *Rangeland Ecol. Manag.* **2013**, *66*, 454–461. [CrossRef]
77. Mikola, J.; Setälä, H.; Virkajärvi, P.; Saarijärvi, K.; Ilmarinen, K.; Voigt, W.; Vestberg, M. Defoliation and Patchy Nutrient Return Drive Grazing Effects on Plant and Soil Properties in a Dairy Cow Pasture. *Ecol. Monogr.* **2009**, *79*, 221–244. [CrossRef]
78. Mazancourt, C.D.; Loreau, M.; Abbadie, L. Grazing Optimization and Nutrient Cycling: When Do Herbivores Enhance Plant Production? *Ecology* **1998**, *79*, 2242–2252. [CrossRef]
79. Luo, G.; Han, Q.; Zhou, D.; Li, L.; Xi, C.; Yan, L.; Hu, Y.; Li, B.L. Moderate Grazing Can Promote Aboveground Primary Production of Grassland under Water Stress. *Ecol. Complex.* **2012**, *11*, 126–136. [CrossRef]